

Taylor & Francis
Taylor & Francis Group

Canadian Journal of Remote Sensing
Journal canadien de télédétection

ISSN: 0703-8992 (Print) 1712-7971 (Online) Journal homepage: www.tandfonline.com/journals/ujrs20

Separating crested wheatgrass using field hyperspectral data in the native prairie of southwestern Saskatchewan

Mohammed , Dale Gross , Yihan Pu , Irini Soubry , Sarula Kang , Xiaomei Li & Xulin Guo

To cite this article: Mohammed , Dale Gross , Yihan Pu , Irini Soubry , Sarula Kang , Xiaomei Li & Xulin Guo (2026) Separating crested wheatgrass using field hyperspectral data in the native prairie of southwestern Saskatchewan, Canadian Journal of Remote Sensing, 52:1, 2654962, DOI: 10.1080/07038992.2026.2654962

To link to this article: https://doi.org/10.1080/07038992.2026.2654962

© 2026 The Author(s). Published by Informa UK Limited, trading as Taylor & Francis Group.

Published online: 15 Apr 2026.

Submit your article to this journal

Article views: 146

View related articles

View Crossmark data

Full Terms & Conditions of access and use can be found at
https://www.tandfonline.com/action/journalInformation?journalCode=ujrs20

CANADIAN JOURNAL OF REMOTE SENSING
2026, VOL. 52, NO. 1, 2654962
https://doi.org/10.1080/07038992.2026.2654962

Taylor & Francis
by informa

OPEN ACCESS Check for updates

Separating crested wheatgrass using field hyperspectral data in the native prairie of southwestern Saskatchewan

Identification de l'agropyre à crête à l'aide de données hyperspectrales de terrain dans la prairie indigène du sud-ouest de la Saskatchewan

Mohammed[a], Dale Gross[b], Yihan Pu[a], Irini Soubry[a], Sarula Kang[a], Xiaomei Li[c], and Xulin Guo[a]

[a]Department of Geography and Planning, University of Saskatchewan, Saskatoon, Saskatchewan, Canada; [b]Landscape Protection Unit, Ministry of Parks, Culture and Sport, Regina, Saskatchewan, Canada; [c]College of Environmental and Resource Sciences & College of Carbon Neutral Modern Industry, Fujian Normal University, Fuzhou, China

ABSTRACT

Crested wheatgrass (*Agropyron cristatum*) is an introduced invasive grass species in North American grasslands. It was initially seeded to increase the grazing duration but is now threatening native grassland biodiversity. In this study we investigated which biophysical and spectral properties (hyperspectral and simulated multispectral) distinguish crested wheatgrass from native grasses. We further assessed whether spectral indices, linked to biophysical traits, could distinguish crested wheatgrass from native grasses. We collected field data of hyperspectral reflectance, leaf area index (LAI), biomass, and vegetation cover. Crested wheatgrass sites have higher grass cover, height, LAI, and biomass (total, live, and dead), but lower bare ground than native grasses. Hyperspectral data showed lower visible and SWIR reflectance for crested wheatgrass than for native grasses. SWIR spectral indices for hyperspectral data, SWIR and visible spectral indices for simulated Sentinel-2A data and visible spectral indices for PlanetScope SuperDove data discriminated crested wheatgrass from native grasses. These findings will advance invasive grass monitoring by shifting the focus from phenology to biophysical properties-based detection, supporting management of crested wheatgrass and restoration of native grassland ecosystems.

RÉSUMÉ

L'agropyre à crête (*Agropyron cristatum*) est une espèce de graminée envahissante introduite dans les prairies nord-américaines. Initialement semée pour prolonger la durée du pâturage, elle menace désormais la biodiversité des prairies indigènes. Cette étude examine les propriétés biophysiques et spectrales (hyperspectrales et multispectrales simulées) qui distinguent l'agropyre à crête des graminées indigènes. Elle évalue également si des indices spectraux, liés à des caractéristiques biophysiques, permettent de différencier l'agropyre à crête des graminées indigènes. Des données de terrain portant sur la réflectance hyperspectrale, l'indice de surface foliaire (ISF), la biomasse et le couvert végétal ont été collectées. Les sites infestés d'agropyre à crête présentent un couvert herbacé, une hauteur, un ISF et une biomasse (totale, vivante et morte) plus élevés, mais une surface de sol nu plus faible que les sites dominés par les graminées indigènes. Les données hyperspectrales révèlent une réflectance visible et infrarouge à ondes courtes (SWIR : ShortWave InfraRed) plus faible pour l'agropyre à crête que pour les graminées indigènes. Les indices spectraux SWIR des données hyperspectrales, les indices spectraux SWIR et visibles des données simulées Sentinel-2A et les indices spectraux visibles des données PlanetScope SuperDove ont permis de distinguer l'agropyre à crête des graminées indigènes. Ces résultats contribueront à améliorer la surveillance des graminées envahissantes en déplaçant l'attention de la phénologie vers une détection basée sur les propriétés biophysiques, ce qui facilitera la gestion de l'agropyre à crête et la restauration des écosystèmes de prairies indigènes.

ARTICLE HISTORY
Received 24 October 2025
Accepted 28 March 2026

KEYWORDS
Crested wheatgrass; hyperspectral remote sensing; invasive grass; spectral indices; simulated multispectral data

CONTACT Mohammed mta401@usask.ca

© 2026 The Author(s). Published by Informa UK Limited, trading as Taylor & Francis Group.
This is an Open Access article distributed under the terms of the Creative Commons Attribution License (http://creativecommons.org/licenses/by/4.0/), which permits unrestricted use, distribution, and reproduction in any medium, provided the original work is properly cited. The terms on which this article has been published allow the posting of the Accepted Manuscript in a repository by the author(s) or with their consent.

Introduction

Crested wheatgrass (*Agropyron cristatum*), an introduced invasive species, is responsible for the degradation of the native grassland ecosystem in the Great Plains of North America (Christian and Wilson 1999; Hansen 2006; Vaness 2008; Zapisocki, Murillo, and Wagner 2022). It was mainly introduced for the revegetation of degraded rangelands and farmlands following severe drought years during the 1930s (Pellant and Lysne 2005; Rogler and Lorenz 1983). It was ideal for this purpose because of its establishment success, resilience to adverse environmental conditions and grazing tolerance (Monsen et al. 2004). Crested wheatgrass can establish in an area with low water availability, quickly stabilizes bare soil and it can produce 1.5 to 2 times more forage than native stands (Ogle 2006). Due to its competitiveness, it hampers the establishment of other invasive species such as Downy Brome (Pellant and Lysne 2005). Additionally, crested wheatgrass is considered good forage for cattle as it greens up early in the spring (Schroeder and Johnson 2019) facilitating its use for early spring grazing (Tandoh 2019). Urness, Austin, and Fierro (1983) reported that crested wheatgrass is also suitable forage for wildlife such as mule deer.

Despite these benefits it presents some ecological challenges. It reduces plant diversity by hampering the establishment and persistence of native plant species, resulting in a monoculture (Davies, Boyd, and Nafus 2013; Henderson and Naeth 2005; Nafus, Svejcar, and Davies 2020; Vaness and Wilson 2007). Available soil moisture beneath crested wheatgrass stands is lower than native species mainly because of its high rate of water usage (Hall, Anderson, and Monsen 1999; Vaness and Wilson 2007). Moreover, crested wheatgrass has a lower root-shoot ratio compared to native plants, leading to a low below-ground carbon storage (Christian and Wilson 1999; Vaness and Wilson 2007). Crested wheatgrass also affects the abundance of fauna species in an ecosystem. For instance, Rockwell et al. (2021) reported that crested wheatgrass presence negatively influenced the abundance of grassland bird species.

To fully harness the potential benefits of an introduced invasive species, such as crested wheatgrass, in a native grassland ecosystem, proper management strategies must be implemented, beginning with the effective monitoring of their spatial distribution. Remote sensing can be an effective means to monitor whether an introduced invasive species is spreading beyond its designated area, and it can be used to assess the effectiveness of management practices, such as mowing, prescribed burning, or herbicide application in controlling or eradicating the species. However, successful application of remote sensing depends on the fact that the invasive species has distinct phenological patterns compared to surrounding native vegetation, unique plant traits, and widespread distribution in the study area (Bolch et al. 2020; Gholizadeh et al. 2022). Some invasive species, such as crested wheatgrass, may exhibit overlapping phenological patterns with other invasive species, such as Smooth Brome. Also, the timing of these phenophases might change with environmental conditions. In both of these cases, distinct biophysical or biochemical plant traits of invasive species can be leveraged to enhance the accuracy of remote detection (Gholizadeh et al. 2022). Spatial and spectral resolution of remote sensing datasets should also be considered to detect invasive plant species of varying patch sizes and traits (Bolch et al. 2020; Müllerová et al. 2023). Specifically, high spatial (e.g., airborne remote sensing) and spectral resolution (e.g., hyperspectral remote sensing) data is a must for accurate detection at the species level (Bolch et al. 2020; Rakotoarivony et al. 2025; Weisberg et al. 2021).

In terms of crested wheatgrass, time and labor-intensive field monitoring approaches (e.g., marker demarcation, plant counting, ground cover photography) are still being suggested (Operation Grassland Community 2022). Only a few studies have tried to detect crested wheatgrass using remote sensing. Zhou (2007) classified crested wheatgrass in the Grassland National Park, Canada by using a single-date (July 27, 2006) SPOT-5 image, with different spectral indices. Even though a high overall accuracy of 79% was achieved, it was concluded that crested wheatgrass was over-classified. Due to the lower spectral resolution of SPOT 5, reflectance of crested wheatgrass was confounded with other vegetation types which resulted in over-classification of crested wheatgrass. Guo et al. (2020) mapped the spatial distribution of crested wheatgrass using visible and shortwave infrared bands of Sentinel-2A data with 70% overall accuracy. They reported some uncertainty in this classification result due to limited field data points and spatial resolution of Sentinel-2A. Similarly, Weisberg et al. (2021) used a

phenology-based classification approach using Unoccupied Aerial Vehicle (UAV) imagery with a 2-cm spatial resolution to distinguish several invasive annual grasses, including crested wheatgrass, to the species level. Their method involved multi-temporal data collection across the growing season (May through July) using a multispectral sensor (Blue, Green, Red, Red Edge, and NIR bands). Although this study achieved high classification accuracy for the target species, cheatgrass (*Bromus tectorum*) and medusahead (*Taeniatherum caput-medusae*), crested wheatgrass was commonly misclassified with medusahead and litter. The authors acknowledged that phenological approaches tend to confuse multiple species due to overlapping phenological characteristics.

Together, these studies highlight a key limitation in existing crested wheatgrass detection efforts: these approaches relied on multispectral or phenology-based methods, which lack the spectral details needed to reliably separate crested wheatgrass from co-occurring species with similar phenological patterns or overlapping spectral signatures. These issues of over-classification, spectral confusion, and inconsistent accuracy emphasize the need for higher spectral resolution data which are needed to identify the subtle spectral regions that reflect species-specific plant characteristics, allowing reliable separation of crested wheatgrass from vegetation that appears spectrally similar in multispectral imagery or phenologically similar in the field. Also, based on our knowledge, there is a lack of studies that have examined the unique biophysical properties of crested wheatgrass, which can help us understand what drives the invasiveness of crested wheatgrass. We address these gaps by using proximal hyperspectral measurements, which offer high spectral resolution and are unaffected by atmospheric and topographic distortions. These data provide precise, continuous spectral profiles that enable the detection of subtle biochemical and structural differences between crested wheatgrass and native grasses. By integrating hyperspectral signatures with biophysical characteristics, our work moves beyond traditional phenology-based approaches and demonstrates a trait-based method for species separation. This overall approach not only clarifies the unique spectral and biophysical characteristics of crested wheatgrass but also identifies spectral indices that can guide the selection of appropriate satellite sensors and inform future large-scale mapping efforts. Therefore, the overall objective of this research is to understand the biophysical and spectral characteristics of crested wheatgrass using field measurements and hyperspectral remote sensing. Specifically, the objectives are: (1) to identify the unique biophysical and spectral characteristics of crested wheatgrass and native grasses using both hyperspectral and simulated multispectral data, and (2) to explore the relationships between spectral indices and the biophysical traits of crested wheatgrass.

Materials and methods

Study area

Saskatchewan Landing Provincial Park (SLPP) (50° 39′ 58″ N, 107° 59′ 23″ W) is situated in the Southwest of the Saskatchewan Province and along the South Saskatchewan River, Canada (Longpre 2024) (Figure 1). This provincial park was established in 1973, and being one of the largest provincial parks in the native prairie region, it encompasses an area of about 57.35 km^2 (Guo et al. 2020). SLPP belongs to the Mixed Grass Prairie ecoregion (Thorpe 2014) and is a unique habitat for a number of different flora and fauna species (Guo et al. 2020). The topography of the park was shaped by deglaciation, and the elevation of this area ranges from 554 m to 708 m, with varying levels of steepness (0% – 92%) (Guo et al. 2020). Between 2000 to 2022, the average annual precipitation was 365.62 mm and the average daily temperature was 4.7 °C (Goverment of Canada 2022). Loamy soil predominates in this region while a small portion of the area is characterized by clay (Guo et al. 2020). The distribution of vegetation communities in the park varies according to topography and soil types (Thorpe 2007). Some of the dominant native grass in this area includes spear grasses (*Hesperostipa comata*, *Nassella viridula*), blue grama grass (*Bouteloua gracilis*), western wheatgrass (*Pascopyron smithii*), and slender wheatgrass (*Elymus trachycaulus*). Sage brush (*Artemisia tridentata*), hybrid cottonwood (*Populus* x *jackii*), Manitoba maple (*Acer negundo*), Trembling aspen (*Populus tremuloides*), Chokecherry (*Prunus virginiana*), Rose (*Rosa spp.*) and Creeping juniper (*Juniperus horizontalis*) are some of the shrub species found in SLPP (Guo et al. 2020). Among the exotic

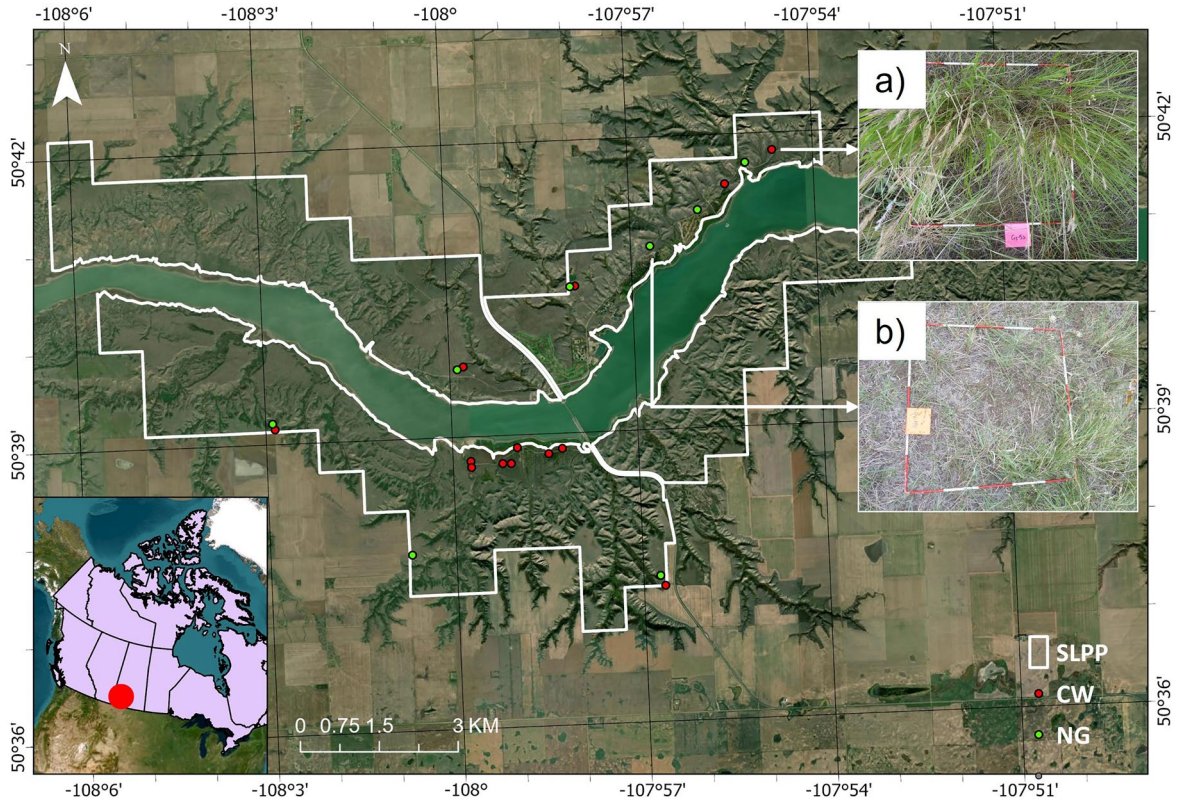


Figure 1. Location of the 21 sampled sites (red and green dots) in Saskatchewan Landing Provincial Park (SLPP) with a true color satellite imagery as background. Quadrats from the crested wheatgrass (a) and native grass (b) plots are shown as examples. (Image source: Esri ArcGIS Pro World Imagery (version dated: 2024-05-09) (ESRI 2025); source of Canadian Provincial boundaries of map: Canada Census Boundary (Canada Statistics 2021); source of SLPP boundary: Saskatchewan Parks Boundaries (Saskatchewan Ministry of Parks Culture and Sports 2021); CW: crested wheatgrass, NG: native grass, and SLPP: Saskatchewan Landing Provincial Park).

species, crested wheatgrass (*Agropyron cristatum*) is the most dominant in SLPP with some dispersion of Smooth brome (*Bromus inermis*) and Kentucky blue grass (*Poa pratensis*) (Godwin and Thorpe 2002; Guo et al. 2020). Moreover, there are different noxious weeds, including Russian knapweed (*Rhaponticum repens*), Canada thistle (*Cirsium arvense*), leafy spurge (*Euphorbia esula*), kochia (*Kochia scoparia*) and common buckthorn (*Rhamnus catharticus*) (Guo et al. 2020).

Field data collection

Field data was collected in late May 2024, when crested wheatgrass typically matures, due to its early spring (late April or early May) growth initiation (Schroeder and Johnson 2019). A total of 21 sites were selected using systematic random sampling approach; 13 sites were situated in crested wheatgrass dominant locations and 8 were in native grass dominated ones. In order to determine crested wheatgrass and native grass dominated sites, species composition and grass cover threshold percentage were used as criteria. If the site has more than 50% coverage, of total vegetation cover, of a grass species (crested wheatgrass or native grass), the site is considered to be dominated by that species. Within each site, two 20 m transects perpendicular to each other were used to collect hyperspectral and biophysical measurements with 50 cm X 50 cm quadrats (referred to as $Q_{(5m,10m)}$ quadrat) along the transects at 5 m intervals (Figure 2). Within each of these quadrats, hyperspectral reflectance, cover percentage of different functional vegetation groups (grass, shrub, forbs, standing dead, litter and bare ground), grass and shrub height (maximum), and leaf area index (LAI) were recorded. Lastly, GPS coordinates of the transect intersection point where collected using a Geo XH 2008 Series Geo Explorer GPS.

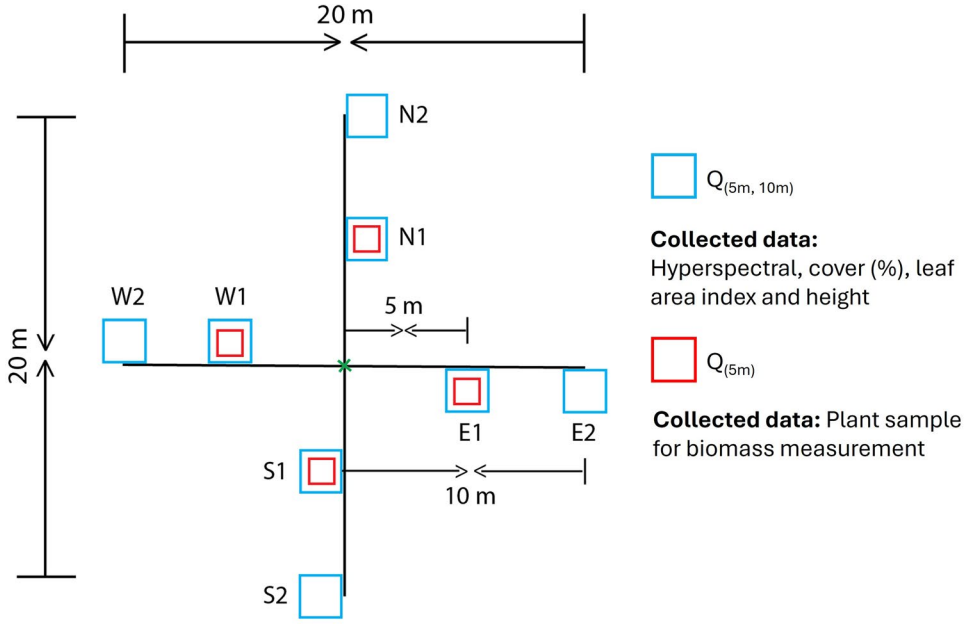


Figure 2. Plot design for data collection across 21 sampling sites, each measuring 20 m x 20 m, in Saskatchewan Landing Provincial Park (SLPP). N, E, W, and S indicate the north, east, west, and south cardinal directions, respectively. Quadrat symbols are schematic and not drawn to scale. The numbers (e.g., $Q_{(5\ m)}$, $Q_{(10\ m)}$) represent the distance of each quadrat from the plot center. The blue and red colored quadrats used for sampling were (50 cm X 50 cm) and (20 cm X 50 cm) in size respectively.

Cover estimation followed the approach used by Daubenmire (1959). When the fractional cover was larger than 5% and smaller than 95%, it was estimated at a 5% increments. When it was below 5% and over 95%, it was estimated at a 1% increment. LAI was measured using a Li-COR LAI-2000, with one above-canopy and five below-canopy measurements, as this sampling intensity was sufficient for accurate site wise LAI calculation (Gordon et al., 1994). The average LAI from 8 quadrats was calculated to represent the LAI value for the site. A Spectroradiometer (ASD FieldSpec Pro) was used to collect field hyperspectral data. This spectroradiometer captures a broad range of wavelengths (350 nm to 2500 nm) that are covered by the visible, shortwave infrared 1 (SWIR1), and shortwave infrared 2 (SWIR2) detectors. It comes with a high spectral resolution of 3 nm within the 350 nm to 1000 nm range and 10 nm at the 1000 nm to 2500 nm range. During field data collection, the spectrometer was held 1 m above ground to record the spectral data from each quadrat with the field of view (FOV) of 25°. The measurements were taken from 10 am to 2 pm during clear sky conditions and with the operator facing the sun to avoid any shadow on the quadrats. A digital picture of each of these 8 quadrats was taken using a digital camera at nadir view.

Above ground biomass harvesting was conducted for four quadrats ($Q_{(5m)}$) of size 20 cm x 50 cm at each site (Xu et al. 2022; Yu et al. 2019). All the vegetation was cut, bagged, and weighed. Sorting took place in the lab to separate green grass, green forb, green shrub, and dead materials. All samples were then dried to weight the dry biomass. All the data (spectral, biomass, vegetation cover, LAI, height) from the $Q_{(5m,10m)}$ and $Q_{(5m)}$ quadrats were averaged to represent the values in their respective sites.

Data analysis

Biophysical properties

A Welch t test (R Core Team 2017) was conducted to investigate the difference between the biophysical properties of crested wheatgrass and native grass for 11 biophysical properties – cover (green grass, standing dead, litter, bare ground, shrub), height, LAI, biomass (green grass, total, dead, and shrub). The biophysical properties that were significantly different were used later during spectral discrimination.

Remote sensing dataset

The field hyperspectral data contain increased noise in wavelength regions affected by strong atmospheric water vapor absorption, which results in a low signal-to-noise ratio (Erudel et al. 2017). Therefore, the water absorption bands (1350–1430 nm, 1750–1980 nm, and 2330–2500 nm) were removed as a preprocessing step to minimize noise and improve spectral reliability (Soubry and Guo 2021). Then, the hyperspectral data were resampled to two multispectral sensors (PlanetScope SuperDove and Sentinel-2A) using their spectral response function information to evaluate the potential application of satellite imagery in discriminating crested wheatgrass. The following formula was used in the resampling process which was adapted from Zheng et al. (2018):

$$R = \int_{\lambda start}^{\lambda end} f(x)\,dx \tag{i}$$

where R is the simulated reflectance of a multispectral band, λend and λstart represents end and start of wavelength (nm) of a band respectively, and f(x) represents the hyperspectral reflectance weighted by the normalized spectral response function of the multispectral sensor. Spectral response functions for Sentinel-2A and PlanetScope SuperDove were obtained from Sentinel (European Space Agency 2025) and PlanetScope (Planet 2025) technical specifications respectively. Reflectance values are unitless.

Welch's t-test was applied to identify spectral regions where reflectance significantly differed ($p < 0.05$) between crested wheatgrass and native grass for the hyperspectral and simulated data. Then, using these significant spectral regions, hyperspectral and simulated multispectral vegetation indices were computed to further assess grass species discrimination (Table 1). Several hyperspectral indices calculated in this study have no direct Sentinel-2A or PlanetScope SuperDove equivalents (Table 1). Using these hyperspectral indices will enable the use of a wider range of indices, including those sensitive to different photosynthetic and carbon compounds, confirming that established hyperspectral indices remain valuable for species discrimination.

Linear model with interaction effect

Initial assessments of biophysical properties and spectral indices using a linear model indicated interactions between crested wheatgrass and native grass across multiple response variables. Therefore, a linear model with interaction effects was applied separately to each of the significant biophysical properties and spectral indices (both hyperspectral and simulated multispectral) combinations (Figure 3). The model assessed whether the relationship between spectral indices (SI) and biophysical properties (BP) varied significantly between species (crested wheatgrass and native grass), with BP as the response variable, species type, SI and their interaction term (species type × SI) as the independent variables for species-wise effects. While the primary goal of using linear model to identify SI and BP associations with significant species-wise differences, we also examined the strength of the associations by analyzing the slope coefficients of the final models.

Results

Biophysical properties of different grassland types

Several biophysical properties are significantly different between crested wheatgrass and native grass including grass and bare ground cover, height, LAI, and biomass (grass, total, and dead) ($p < 0.05$) (Table 2). Except for bare ground cover, all the other biophysical properties were significantly higher for crested wheatgrass. Coefficient variation assessment indicated that crested wheatgrass had lower spatial variation for most of the biophysical variables (Table 2).

Spectral properties of different grassland types

Native grass had higher spectral reflectance compared to crested wheatgrass in the visible, shortwave infrared (SWIR), and some parts of the NIR region (Figure 4), according to the hyperspectral data.

Table 1. List of Hyperspectral indices used in this study.

Properties	Hyperspectral indices	Equation	Citation	Sentinel-2A equivalent	PlanetScope SuperDove equivalent
Pigment	Normalized Differenced Vegetation indices (682-553) (NDVI, NDVIS2, NDVIPS)	$(R_{682} - R_{553}) / (R_{682} + R_{553})$	(Gandia et al. 2004)	$(R_{B4} - R_{B3}) / (R_{B4} + R_{B3})$	$(R_{B6} - R_{B4}) / (R_{B6} + R_{B4})$
	Carotenoid Reflectance Index I (CRI 1, CRIS2, CRIPS)	$(1/R_{510}) - (1/R_{550})$	(Gitelson et al. 2002; Hill 2013)	$(1/R_{B2}) - (1/R_{B3})$	$(1/R_{B2}) - (1/R_{B3})$
	Red Green Ratio (RGR, RGRS2, RGRPS)	$x = \frac{\sum_{600}^{699} Ri}{\sum_{500}^{599} Ri}$	(Hill 2013; Sims and Gamon 2002)	R_{B4}/R_{B3}	R_{B6}/R_{B4}
	Photochemical reflectance index (PRI, PRIPS)	$(R_{531} - R_{570}) / (R_{531} + R_{570})$	(Sims and Gamon 2002)	NA	$(R_{B3} - R_{B4})/ (R_{B3} + R_{B4})$
	Anthocyanin Reflectance Index I (ARI 1)	$(1/R_{550}) - (1/R_{700})$	(Gitelson, Merzlyak, and Chivkunova 2001)	NA	NA
	Simple Ratio (SR)	R_{700} / R_{670}	(Hill 2013; Nagler et al. 2003)	NA	NA
	Modified Chlorophyll Absorption Ratio Index 2 (MCARI2)	$((R_{700} - R_{670}) - 0.2 * (R_{700} - R_{550})) * (R_{700} - R_{670})$	(Daughtry 2000)	NA	NA
	Transformed Chlorophyll Absorption Reflectance Index (TCARI)	$3 * ((R_{700} - R_{670}) - 0.2 * (R_{700} - R_{550})) * (R_{700} / R_{670})$	(Daughtry 2000)	NA	NA
	Simple ratio pigment index (SRPI)	R_{430}/R_{680}	(Penuelas, Baret, and Filella 1995)	NA	NA
Biochemical properties	Cellulose Absorption Index (CAI, CAIS2)	$((R_{2000} + R_{2200}) / 2) - R_{2100}$	(Hill 2013; Nagler et al. 2003)	R_{B12}/R_{B11}	NA
	Normalized Difference Nitrogen Index (NDNI)	$(\log(1/R_{1510}) - \log(1/R_{1680})) / (\log(1/R_{1510}) + \log(1/R_{1680}))$	(Serrano, Peñuelas, and Ustin 2002)	NA	NA
Stress indicator	Yellowness Index (YI, YIPS)	$(R_{567-587} - 2R_{616-636} + R_{656-676}) / \Delta\lambda^2$	(Adams, Philpot, and Norvell 1999; Tu et al. 2022)	NA	$(R_{GreenII} - 2R_{Yellow} + R_{Red}) / \Delta\lambda^2$
	Water Stress Index (WSI, WSIS2)	R_{1660}/R_{550}	(Apan et al. 2004)	R_{B11}/R_{B3}	NA
Structural properties	Shortwave-Infrared Vegetation Index (SWVI)	$37.72 * (R_{2210} - R_{2090}) + 26.27 * (R_{2280} - R_{2090}) + 0.57$	(Lobell et al. 2001)	NA	NA
	Soil Adjusted Total Vegetation Index (SATVI, SARVIS2)	$((R_{1650} - R_{680})/(R_{1650} + R_{680} + L))(1 + L) - R_{2215}/2$	(Marsett et al. 2006)	$((R_{B11} - R_{B4}) / (R_{B11} + R_{B4} + L)) * (1 + L) - (R_{B12} / 2)$	NA
	Hyperspectral biomass and structural index (HVSIS2)	NA	(Thenkabail et al. 2013)	$(R_{B11} - R_{B4}) / (R_{B11} + R_{B4})$	NA

In this table, "R" represents reflectance and preceding numbers following R indicate wavelengths in nm. Simulated multispectral indices are identified by adding the satellite name to the index (PlanetScope SuperDove: PS; Sentinel-2A: S2), for example RGR, RGRPS, and RGRS2.

Statistical results showed that crested wheatgrass and native grass had significantly different spectral reflectance in the visible (390–700 nm) and the SWIR (1430–1749 nm and 1981–2329 nm) regions ($p < 0.05$) (Figure 4). Based on these unique hyperspectral regions, 15 hyperspectral indices were calculated (Table 1) to represent different biophysical properties.

The simulated Sentinel-2A and PlanetScope SuperDove spectral data showed the same patterns as the hyperspectral data (Figure 5). Reflectance in the coastal blue and visible (blue, green I, green II, red and yellow) bands differed significantly between crested wheatgrass and native grass ($p < 0.05$) for simulated PlanetScope SuperDove data (Figure 5). For simulated Sentinel-2A, the coastal aerosol, visible (blue, green and red) and shortwave infrared (SWIR1 and SWIR 2) bands showed noticeable differences in reflectance between the two grass types ($p < 0.05$) (Figure 5). Using the significant bands, five simulated PlanetScope SuperDove spectral indices and seven simulated Sentinel-2A indices (Table 1) were calculated, all of which (except for one Sentinel-2A index: Hyperspectral biomass and structural index) were adapted from the calculated hyperspectral indices.

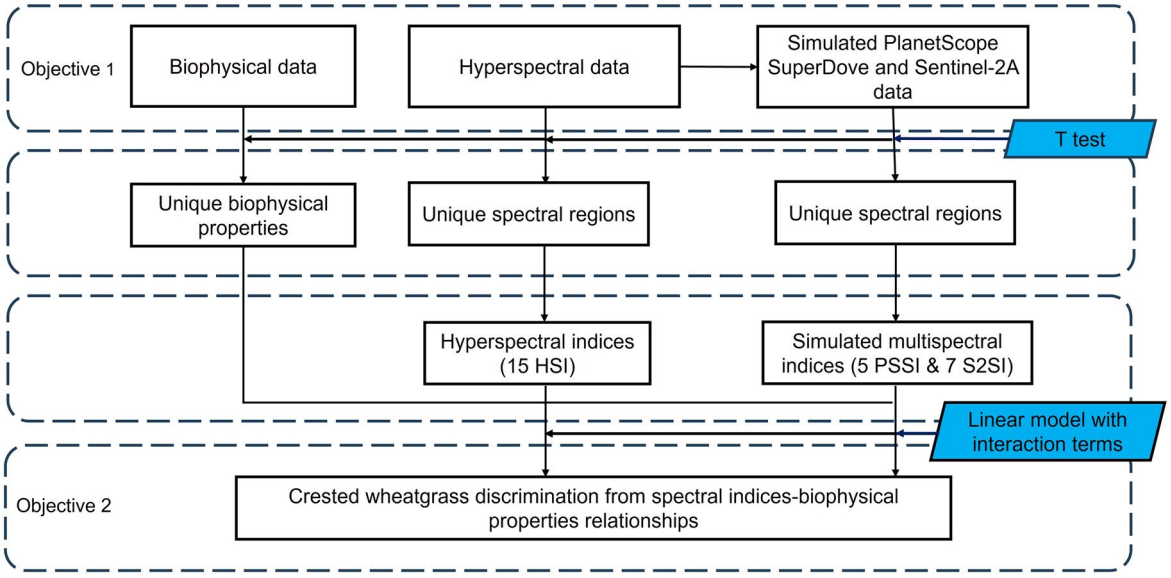


Figure 3. Workflow summarizing the steps from biophysical and spectral data collection to crested wheatgrass separation using linear models.

Table 2. Descriptive statistics of biophysical properties of crested wheatgrass and native grass.

	Mean (Std)			Coefficient of variation	
Biophysical properties	Crested wheatgrass	Native grass	p	Crested wheatgrass	Native grass
Grass cover (%)	40 (8.4)	23 (3.5)	<0.001	0.21	0.15
Standing dead cover (%)	11 (5.3)	9 (4.5)	Not significant	0.48	0.49
Litter cover (%)	45 (8.4)	48 (9.1)	Not significant	0.19	0.19
Bare ground (%)	2 (3.8)	8 (4.6)	<0.01	0.167	0.56
Shrub cover (%)	1 (1.9)	2.5 (2.7)	Not significant	0.201	0.108
Height (cm)	40.5 (4.1)	22.3 (3.5)	<0.001	0.10	0.16
Leaf area index	1.7 (0.5)	1.0 (0.19)	<0.001	0.27	0.19
Grass biomass (gm/m^2)	150.7 (50.0)	75.5 (29.8)	<0.01	0.33	0.39
Total Biomass (gm/m^2)	356.9 (96.7)	224.0 (80.6)	<0.01	0.27	0.35
Dead biomass (gm/m^2)	194.5 (67.4)	130.6 (60.4)	<0.05	0.35	0.46
Shrub biomass (gm/m^2)	10.6 (17.4)	7.0 (9.0)	Not significant	0.165	0.128

Crested wheatgrass discrimination using a linear model with interaction

Clear interactions can be observed when estimating biophysical properties using spectral data for crested wheatgrass and native grass (Figure 6) using hyperspectral indices. We selected those with the strongest species-specific pattern (lowest p-value for the species type × SI interaction term) for the relationship between biophysical properties and spectral indices (Table 3). The Height–Shortwave Vegetation Index (SWVI) (p_{int} = 0.005), Grass biomass–Cellulose Absorption Index (CAI) (p_{int} = 0.002), Total biomass–CAI (p_{int} = 0.021), and Leaf area index–CAI (p_{int} = 0.003) model showed a negative association between biophysical properties and spectral indices for crested wheatgrass, while opposite pattern was observed for native grass. However, in the Bare ground cover–CAI (p_{int} = 0.007) model, crested wheatgrass and native grass showed opposing patterns compared to the other four models (Figure 6 and Table 3).

Similar interactions were revealed using the simulated PlanetScope SuperDove indices (Figure 7 and Table 3). In the Grass cover–Photochemical reflectance index PlanetScope SuperDove (PRIPS) (p_{int} = 0.007), LAI–Red green ratio PlanetScope SuperDove (RGRPS) (p_{int} = 0.028) and Total biomass–RGRPS (p_{int} = 0.019) models, the biophysical properties of crested wheatgrass were inversely associated with the spectral indices, contrasting with the positive association observed in native grass (Figure 7 and Table 3). For the Grass cover–PRIPS and LAI–RGRPS (p_{int} = 0.028) model, biophysical properties of native grasses showed minimal response to variations in spectral indices (Figure 7).

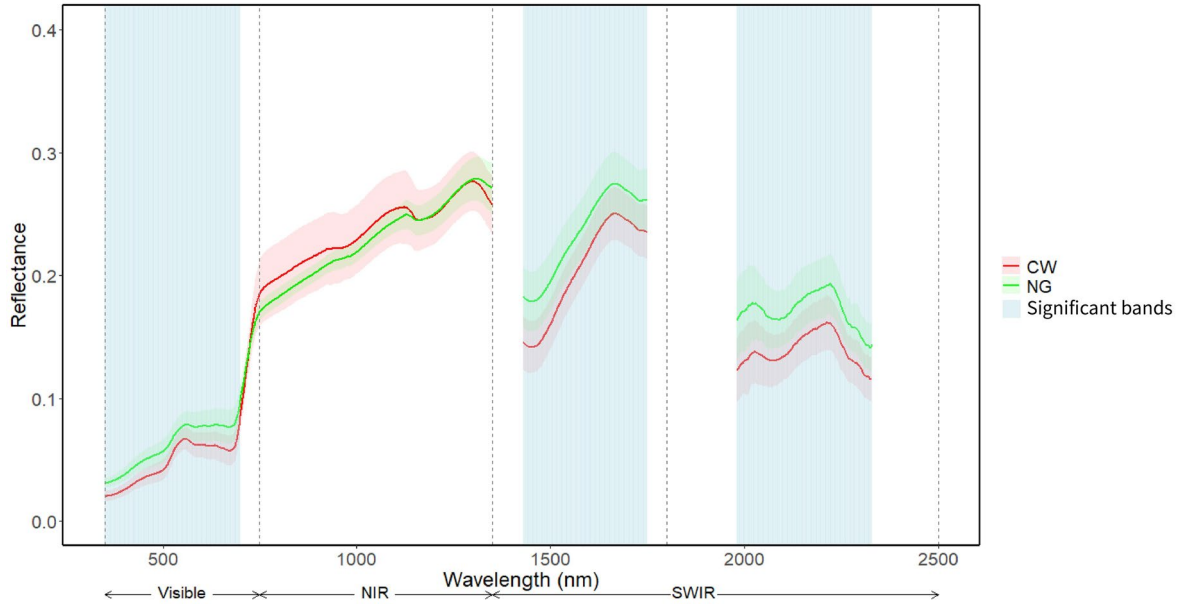


Figure 4. Mean spectral profile of crested wheatgrass and native grass collected by field spectroradiometer. Blue shaded regions indicate significant differences ($p < 0.05$) between crested wheatgrass and native grass reflectance.

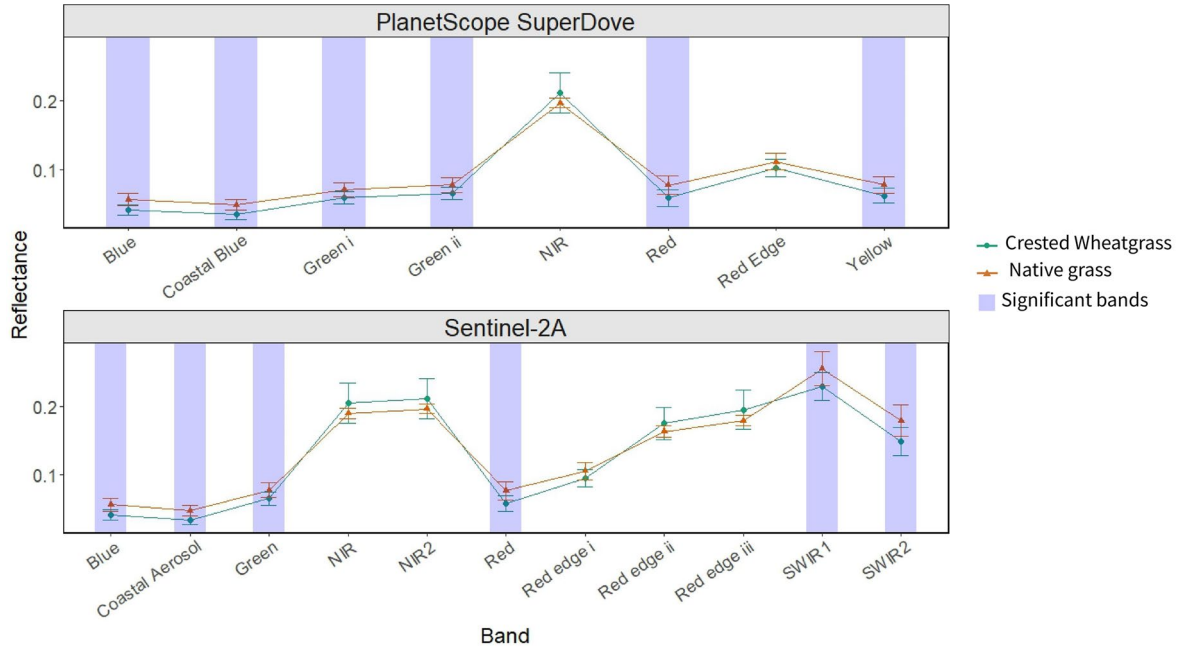


Figure 5. Simulated PlanetScope SuperDove and Sentinel-2A spectral data. Blue shaded regions indicate significant differences ($p < 0.05$) between crested wheatgrass and native grass reflectance (larger font size).

However, for the Bare ground cover–RGRPS model, bare ground in crested wheatgrass plots increased with RGRPS values, whereas native grasses showed a negative trend (Figure 7 and Table 3).

Similarly, using the simulated Sentinel-2A spectral indices, three linear models stood out as having the strongest species-wise pattern (Table 3). The total biomass and LAI values decreased with the respective spectral index values for crested wheatgrass in the Total biomass–Red green ratio Sentienl-2A (RGRS2) and Leaf area index–RGRS2 model respectively (Figure 8 and Table 3). But total biomass showed positive association with RGRS2 for native grass and LAI remained constant (Figure 8 and Table 3). Conversely, the Bare ground cover–Water stress index Sentienl-2A (WSIS2) models revealed opposing patterns for crested wheatgrass and native grass compared to the first two models (Figure 8 and Table 3).

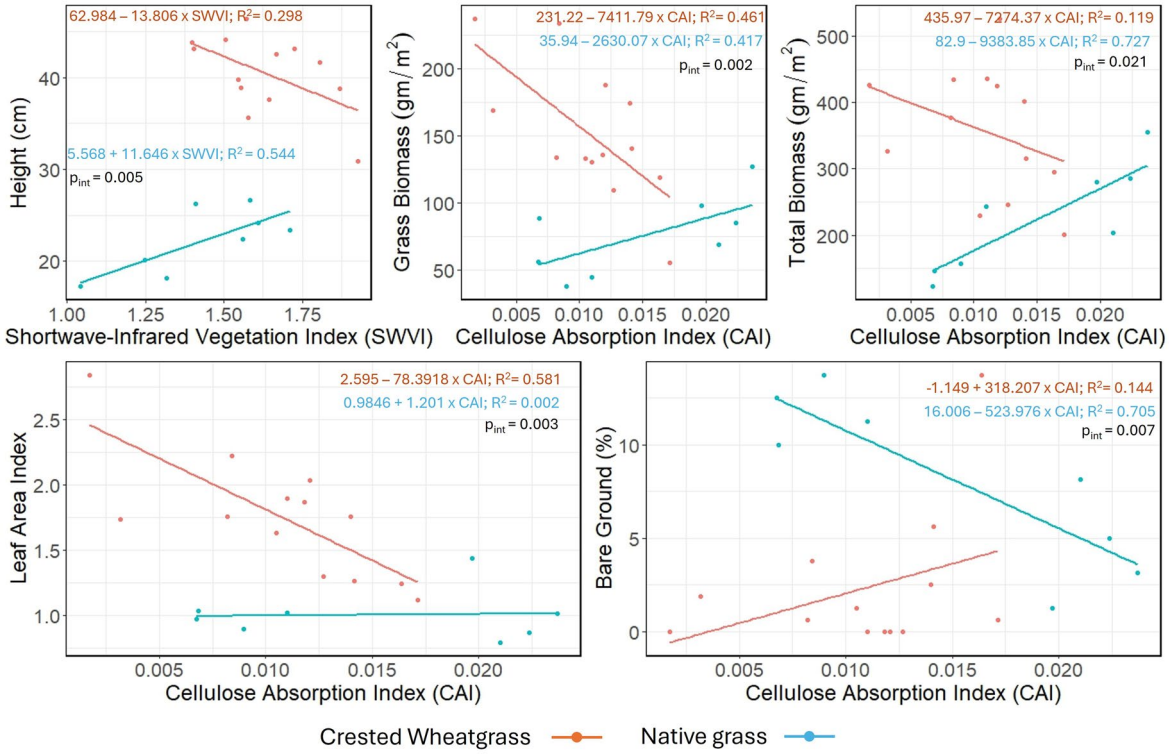


Figure 6. Result of linear regression models with interaction showing the slope difference (p_{int}) between the relationship of hyperspectral indices and biophysical properties. $p_{int} < 0.05$ indicates a significant difference between the slopes of crested wheatgrass and native grass.

Table 3. Results of the significant linear regression models show the interaction between species (crested wheatgrass =0, native grass =1) through the slope difference (p_{int}), the variance explained (R^2), and the linear equation for the models assessing the relationship between various spectral indices and biophysical properties.

Biophysical properties (Dataset type)	Equation ($\beta_0 + \beta_1$ x Spectral indices + β_2 x Species + β_3 x (Spectral indices x Species))	R^2	p_{int}
Height (Hyperspectral)	62.98 – 13.80 × SWVI – 57.41 × Species + 25.45 × (SWVI × Species)	0.904	0.005
Grass biomass (Hyperspectral)	231.22 – 7411.79 × CAI – 195.28 × Species + 10041.86 × (CAI × Species)	0.692	0.002
Total biomass (Hyperspectral)	435.97 – 7274.37 × CAI – 353.07 × Species + 16658.22 × (CAI × Species)	0.546	0.02
Total biomass (PlanetScope SuperDove)	718.70 – 405.80 × RGRPS –79.33 × Species + 1579.60 × (RGRPS × Species)	0.539	0.019
Total biomass (Sentinel-2A)	702.60 – 391.20 × RGRS2 – 1561.20 × Species + 1485.70 × (RGRS2 × Species)	0.538	0.02
Leaf area index (Hyperspectral)	2.59 – 78.39 × CAI – 1.61 × Species + 79.59× (CAI × Species)	0.756	0.003
Leaf area index (PlanetScope SuperDove)	5.86 – 4.62 × RGRPS –4.80 × Species + 4.56 × (RGRPS × Species)	0.806	0.028
Leaf Area Index (Sentinel-2A)	5.63 – 4.40 × RGRS2 – 4.55 × Species + 4.3279 × (RGRS2 × Species)	0.808	0.027
Bare ground cover (Hyperspectral)	–1.14 + 318.20 × CAI + 17.15 × Species – 842.18 × (CAI × Species)	0.602	0.007
Bare Ground (PlanetScope SuperDove)	–18.55 + 23.41× RGRPS +72.36 × Species –69.57× (RGRPS × Species)	0.533	0.022
Bare ground cover (Sentinel-2A)	–19.18 + 6.10× WSIS2 + 50.55 × Species – 13.07× (WSIS2 × Species)	0.528	0.022
Grass Cover (PlanetScope SuperDove)	–86.95 – 2534.98 × PRIPS – 94.99 × Species + 2211.13 × (PRIPS × Species)	0.839	0.007

Discussion

Several studies have combined plant biophysical properties with spectral signatures to discriminate invasive vegetation species (Gholizadeh et al. 2022; Mallmann et al. 2023; Rakotoarivony et al. 2023). Building on this approach, this study identified unique biophysical and spectral characteristics of

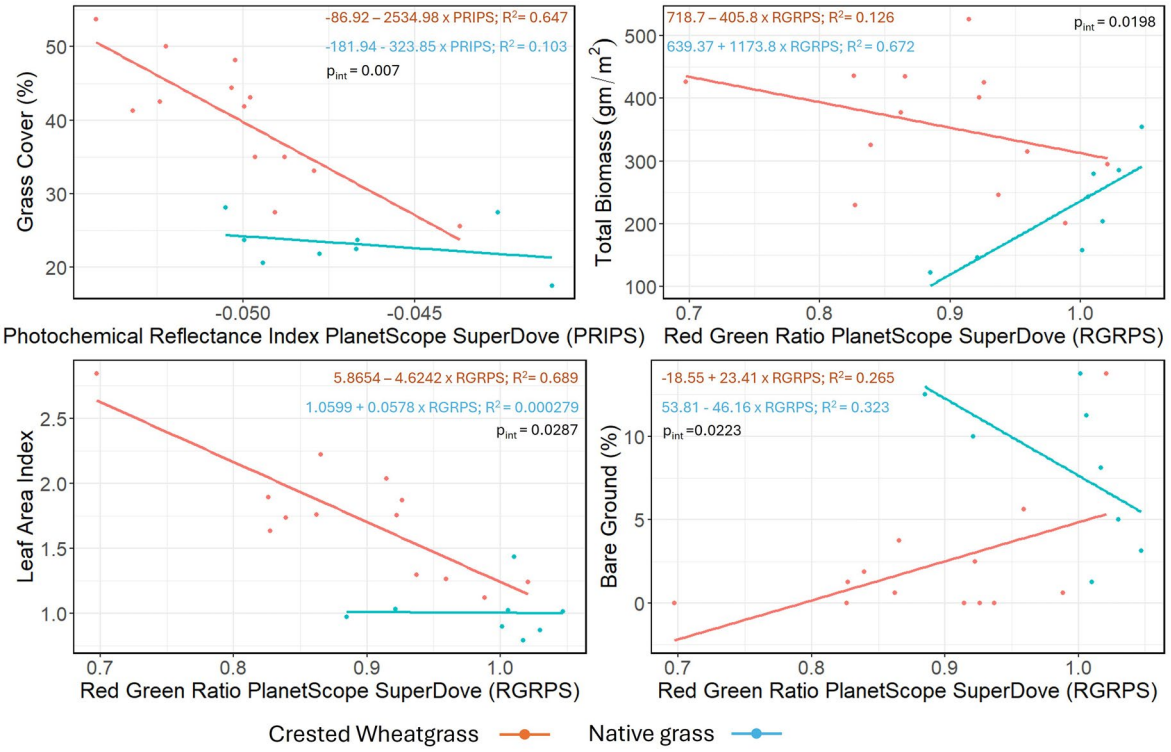


Figure 7. Result of linear regression models with interaction showing the slope difference (p_{int}) between the relationship of simulated PlanetScope SuperDove spectral indices and biophysical properties. $p_{int} < 0.05$ indicates a significant difference between the slopes of crested wheatgrass and native grass.

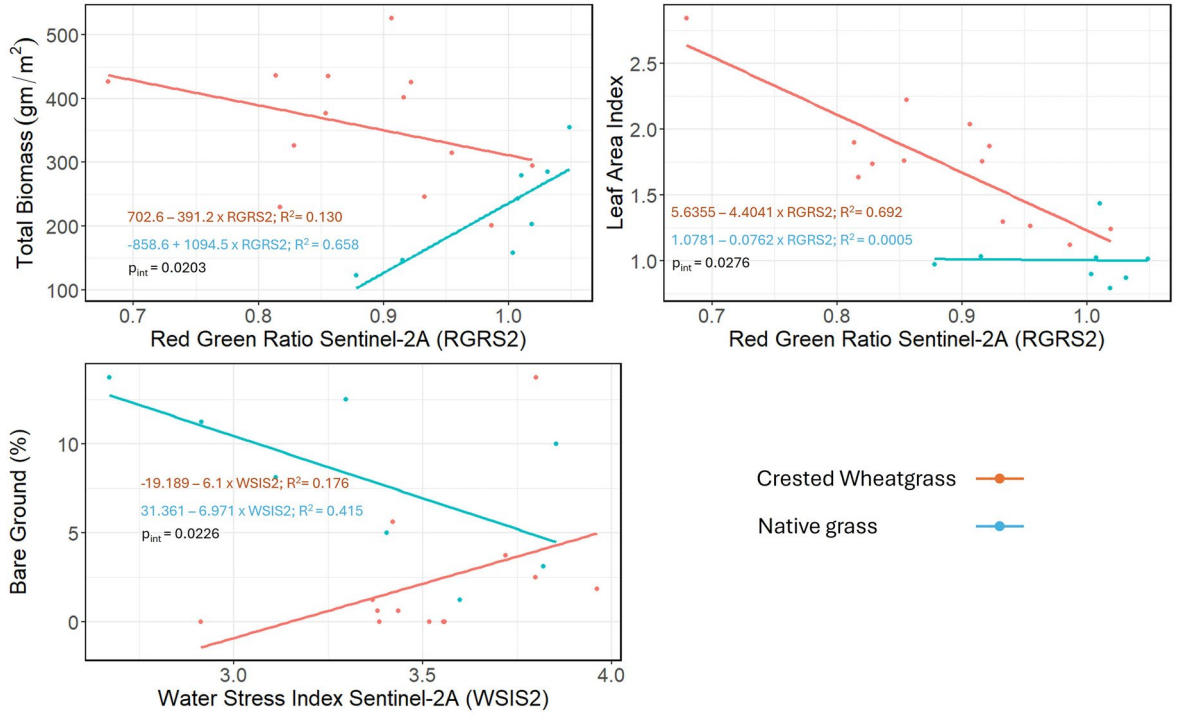


Figure 8. Result of linear regression model with interaction showing the slope difference (p_{int}) between the relationship of simulated Sentinel-2A spectral indices and biophysical properties. $p_{int} < 0.05$ indicates a significant difference between the slopes of crested wheatgrass and native grass.

crested wheatgrass using hyperspectral data and simulated multispectral data and related these variables to effectively distinguish crested wheatgrass from native vegetation.

Biophysical differences explain crested wheatgrass dominance

We found that seven biophysical properties showed significant differences between the two grass type groups and except for the bare ground cover, all the biophysical properties are higher for crested wheatgrass (Table 2). These results could provide an understanding of which biophysical properties facilitate competition, establishment, and spread mechanisms of crested wheatgrass. For instance, the tall and dense structure of crested wheatgrass might hamper the establishment of other surrounding vegetation that are shade intolerant, which in turn may lead to high dominance of crested wheatgrass and low diversity in the stand (Vojtech, Turnbull, and Hector 2007). Further, this tall stature of crested wheatgrass may help it to capture more light, thus leading to higher overall biomass and leaf area construction (Irving 2015; Pérez-Harguindeguy et al. 2016; Wu et al. 2024). This also substantiates the result that we found for the higher biomass and LAI of crested wheatgrass in this study (Table 1). Christian and Wilson (1999) and Nafus et al. (2015) observed a similar result showing that crested wheatgrass had a higher abundance compared to other vegetation. However, Davies, Bates, and Boyd (2023) found that crested wheatgrass abundance did not significantly increase after a seven-year period compared to other vegetation cover. The greater cover, biomass, height, and leaf area index of crested wheatgrass likely contributed to the lower bare ground observed in this study. Henderson (2005) reported a relationship between the presence of crested wheatgrass and bare ground cover, noting that the removal of crested wheatgrass led to an increase in bare ground. However, it depended on the site-specific conditions. At our study site, the naturally dry native grasslands tend to have higher exposed bare soil. Additionally, older crested wheatgrass stands or those that did not establish well after seeding have gaps in vegetation, resulting in higher bare ground cover. Therefore, bare ground cover alone might not be a reliable indicator of crested wheatgrass presence. In a stressed ecosystem, loss of crested wheatgrass might lead to occupation of the bare ground by weeds or exotic annuals (Davies, Boyd, and Nafus 2013).

Spectral separation of crested wheatgrass

In this study, the visible and SWIR hyperspectral regions were able to separate crested wheatgrass from native grass (Figure 4). Generally, the spectral reflectance pattern for vegetation is similar for all plant species within the 350-2500nm spectral range (Bruning et al. 2020). Throughout the visible region the plant reflectance (specifically, in the blue and red regions) can be limited by the presence of photosynthetic pigments such as chlorophyll, carotenoids, etc. (Blackburn 2007; Bruning et al. 2020). In our study, crested wheatgrass showed a significantly lower reflectance in the visible range (Figure 4) which might be explained by the higher absorption of light by these pigments compared to native grass. More specifically, in the blue (400–500 nm) and red region (650-700nm) the difference in reflectance is more prominent, as these two regions are more sensitive to the presence of chlorophyll and carotenoid (Bruning et al. 2020), compared to the green bands. This suggests crested wheatgrass contains more photosynthetic pigments than the native grass.

In the NIR region, which lacks a strong absorption feature (Ollinger 2011), reflectance is governed by leaf cell structure, leaf development and light scattering (Sahoo, Ray, and Manjunath 2015). Our statistical results indicate that there are no notable differences in the NIR regions (Table 2) and thus this might indicate that both crested wheatgrass and native grass have similar leaf internal and external structural properties. Additionally, crested wheatgrass reflectance was significantly lower in the SWIR regions (Table 2). Vegetation water content and biochemical components such as protein, cellulose, lignin, and starch dictate the plant reflectance in the SWIR spectral region (Bruning et al. 2020; Sahoo, Ray, and Manjunath 2015). Therefore, our result is indicative of comparatively higher leaf water and biochemical component in crested wheatgrass compared to native grass. The higher biomass values of crested wheatgrass also corroborate this assumption (Table 2).

Similar patterns to hyperspectral data were observed for the simulated PlanetScope SuperDove and Sentinel-2A data. We found that six PlanetScope SuperDove and seven Sentinel-2A bands discriminated crested wheatgrass from native grass (Figure 5). Even though the simulated multispectral data were able to separate crested wheatgrass using certain bands, they don't represent the spaceborne satellite conditions properly as satellite remote sensing data is affected by atmospheric interference and topographic effects (Taylor, Hill, and Edwards 2013). Additionally, PlanetScope SuperDove and Sentinel-2A capture data at three and ten meter spatial resolution respectively, and each pixel is a mixture of different covers (grass, bare ground, forbs, shrub). The spectral information that is obtained from the satellite data will be different from the simulated multispectral result. Since multispectral data have much broader spectral information, separation of crested wheatgrass from other invasive species (such as Smooth Brome), which have similar phenology, might be difficult. As a result, discrimination of crested wheatgrass from the native species might be confounded.

Spectral and biophysical relationships separating crested wheatgrass

For the hyperspectral data, the SWVI and CAI based models were able to discriminate crested wheatgrass from native grass (Figure 6 and Table 3). The SWVI is based on three bands situated in the SWIR range (Table 1), which is highly sensitive to water and cellulose content (Bruning et al. 2020; Sahoo, Ray, and Manjunath 2015). This might be an indication that crested wheatgrass and native grass have different levels of moisture and cellulose content. Similarly, CAI also consists of bands from the SWIR range and indicates a similar distinction of moisture and cellulose content. As previously emphasized, because of the importance of reflectance in the SWIR range for discriminating crested wheatgrass, it can be inferred that SWIR-based spectral indices may be effective in separating crested wheatgrass from other vegetation.

On the other hand, among the PlanetScope SuperDove spectral indices, the PRIPS and RGRPS separated crested wheatgrass from native grass in their association with grass cover, total biomass, LAI and bare ground cover (Figure 7 and Table 3). PRIPS is computed with the two green bands of PlanetScope SuperDove data and is used as both stress indicator and pigment estimator (Sims and Gamon 2002). And, the association of RGRPS with the biophysical properties represent contrasting photosynthetic pigment level between crested wheatgrass and native grass plots (Figure 7).

Sentinel-2A based RGRS2 and WSIS2 were able discriminate crested wheatgrass when they are associated with total biomass, and LAI and bare ground respectively (Figure 8 and Table 3). The RGRS2 is based on the red and green bands (Table 1), which are sensitive to photosynthetic pigments and might indicate two different pigment concentration levels of crested wheatgrass and native grass. The WSIS2 indicates plant stress (Apan et al. 2004), and consists of reflectance from the SWIR1 and Green bands. Crested wheatgrass and native grass are showing contrasting associations for WSIS2 and bare ground cover indicating that the stress levels are different for each species (Figure 8). This pattern is consistent with the field observations, which revealed that native grass sites generally have more forbs, shrubs, exposed soil, and less green grass cover compared to the crested wheatgrass sites.

Future work

Our findings provide a foundation for future work aimed at mapping crested wheatgrass using hyperspectral and multispectral satellite imageries. The spectral–biophysical relationships identified here indicate spectral regions and indices most promising for distinguishing crested wheatgrass from native grass communities. Future studies could build on these results by using these discriminative spectral indices from satellite hyperspectral imagery in supervised classification models. Incorporating multi-temporal satellite imagery to capture the unique phenology of crested wheatgrass, as well as testing data with different spatial and temporal resolutions, would further enhance model performance (Pu et al. 2025; Rakotoarivony et al. 2025). Building on the findings of this study, a subsequent study has successfully mapped the spatial distribution of crested wheatgrass using the multispectral indices identified here (Gross et al. 2026). Additionally, expanding field sampling across multiple seasons

would improve the representativeness of the biophysical and spectral data and would support the use of other nonlinear regression approaches to better characterize biophysical–spectral relationships, thereby enhancing the robustness and generalizability of classification models.

Conclusions

We found crested wheatgrass had distinct grass cover, height, total biomass, grass biomass, bare ground cover, LAI and dead biomass, compared to native grass. Additionally, reflectance in the visible and short-wave infrared regions, of hyperspectral and simulated multispectral data, separated crested wheatgrass from native grass. Lastly, models with SWIR spectral indices (SWVI and CAI) for hyperspectral data, SWIR and visible spectral indices (RGRS2 and WSIS2) for simulated Sentinel-2A data and visible spectral indices (RGRPS and PRIPS) for PlanetScope SuperDove data were able to discriminate crested wheatgrass from native grass. The spectral indices identified in this study can be used to map crested wheatgrass over a larger scale using imaging remote sensing systems. However, the simulated Sentinel-2A and PlanetScope SuperDove spectral indices have to be tested with satellite data as the simulated data do not account for the atmospheric and topographic distortion that might be present in satellite data. Limiting field data to the early growing season may restrict the representation of crested wheatgrass, whereas multi-temporal field data would provide a more complete picture. Overall, these results can be useful for mapping the spatial distribution of crested wheatgrass, applying management strategies, and restoring native grasslands. It could also facilitate the assessment of different management practices.

Acknowledgements

The authors would like to acknowledge Yunpei Lu and Saskatchewan Landing Provincial Park authority for their assistance with field data collection.

Author contributions

CRediT: **Mohammed**: Conceptualization, Data curation, Formal analysis, Investigation, Methodology, Visualization, Writing – original draft, Writing – review & editing; **Dale Gross**: Conceptualization, Data curation, Writing – original draft, Writing – review & editing; **Yihan Pu**: Data curation, Writing – review & editing; **Irini Soubry**: Formal analysis, Writing – review & editing; **Sarula Kang**: Data curation, Writing – review & editing; **Xiaomei Li**: Data curation, Writing – review & editing; **Xulin Guo**: Data curation, Formal analysis, Funding acquisition, Investigation, Supervision, Writing – original draft, Writing – review & editing.

Disclosure statement

No potential conflict of interest was reported by the author(s).

Funding

This research was funded by Natural Sciences and Engineering Research Council of Canada (NSERC), grant number RGPIN-201603960.

Data availability statement

The raw data supporting the conclusions of this article will be made available by the author (Mohammed) on request.

References

Adams, M.L., Philpot, W.D., and Norvell, W.A. 1999. "Yellowness index: An application of spectral second derivatives to estimate chlorosis of leaves in stressed vegetation." *International Journal of Remote Sensing*, Vol. 20 (No. 18):pp. 3663–3675. doi:10.1080/014311699211264.

Apan, A., Held, A., Phinn, S., and Markley, J. 2004. "Detecting sugarcane 'orange rust' disease using EO-1 Hyperion hyperspectral imagery." *International Journal of Remote Sensing*, Vol. 25 (No. 2):pp. 489–498. doi:10.1080/01431160310001618031.

Blackburn, G.A. 2007. "Hyperspectral remote sensing of plant pigments." *Journal of Experimental Botany*, Vol. 58 (No. 4):pp. 855–867. doi:10.1093/jxb/erl123.

Bolch, E. A., Santos, M. J., Ade, C., Khanna, S., Basinger, N. T., Reader, M. O., and Hestir, E. L. 2020. "Remote Detection of Invasive Alien Species." In *Remote Sensing of Plant Biodiversity*, pp. 267–307. Cham, Switzerland: Springer International Publishing. doi:10.1007/978-3-030-33157-3_12.

Bruning, B., Berger, B., Lewis, M., Liu, H., and Garnett, T. 2020. "Approaches, applications, and future directions for hyperspectral vegetation studies: An emphasis on yield-limiting factors in wheat." *Plant Phenome Journal*, Vol. 3 (No. 1):pp. 1–22. doi:10.1002/ppj2.20007.

Canada Statistics. 2021. "Canada census boundary."

Christian, J.M., and Wilson, S.D. 1999. "Long-Term Ecosystem Impacts of an Introduced Grass in the Northern Great Plains." *Ecology*, Vol. 80 (No. 7):pp. 2397–2407. doi:10.2307/176919.

Daubenmire, R.F. 1959. "A canopy-coverage method of vegetational analysis." *Northwest Science*, Vol. 33 pp. 43–64.

Daughtry, C. 2000. "Estimating corn leaf chlorophyll concentration from leaf and canopy reflectance." *Remote Sensing of Environment*, Vol. 74 (No. 2):pp. 229–239. doi:10.1016/S0034-4257(00)00113-9.

Davies, K.W., Bates, J.D., and Boyd, C.S. 2023. "Is Crested Wheatgrass Invasive in Sagebrush Steppe with Intact Understories in the Great Basin?" *Rangeland Ecology & Management*, Vol. 90 pp. 322–328. doi:10.1016/j.rama.2023.03.004.

Davies, K.W., Boyd, C.S., and Nafus, A.M. 2013. "Restoring the sagebrush component in crested wheatgrass-dominated communities." *Rangeland Ecology & Management*, Vol. 66 (No. 4):pp. 472–478. doi:10.2111/REM-D-12-00145.1.

Erudel, T., Fabre, S., Houet, T., Mazier, F., and Briottet, X. 2017. "Criteria Comparison for Classifying Peatland Vegetation Types Using In Situ Hyperspectral Measurements." *Remote Sensing*, Vol. 9 (No. 7):pp. 748. doi:10.3390/rs9070748.

ESRI. 2025. Esri ArcGIS Pro World Imagery [WWW Document]. https://services.arcgisonline.com/ArcGIS/rest/services/World_Imagery/MapServer (accessed 1.12.25).

European Space Agency. 2025. Sentinel-2 Spectral Response Functions (S2-SRF) [WWW Document]. https://sentinels.copernicus.eu/web/sentinel/search?p_p_id=com_liferay_portal_search_web_search_results_portlet_SearchResultsPortlet_INSTANCE_XIxtnlMxlnwC&p_p_lifecycle=0&p_p_state=maximized&p_p_mode=view&_com_liferay_portal_search_web_search_results_port (accessed 5.15.25).

Gandia, S., Fernández, G., García, J. C., and Moreno, J. 2004. "Retrieval of vegetation biophysical variables from CHRIS/PROBA data in the SPARC campaign." *European Space Agency, (Special Publication) ESA SP*, (No. 578), pp. 40–48. Noordwijk, The Netherlands: European Space Agency.

Gholizadeh, H., Friedman, M.S., McMillan, N.A., Hammond, W.M., Hassani, K., Sams, A.V., Charles, M.D., *et al.* 2022. "Mapping invasive alien species in grassland ecosystems using airborne imaging spectroscopy and remotely observable vegetation functional traits." *Remote Sensing of Environment*, Vol. 271, pp. 112887. doi:10.1016/j.rse.2022.112887.

Gitelson, A.A., Merzlyak, M.N., and Chivkunova, O.B. 2001. "Optical properties and nondestructive estimation of anthocyanin content in plant leaves." *Photochemistry and Photobiology*, Vol. 74 (No. 1), pp. 38. doi:10.1562/0031-8655(2001)074<0038:OPANEO>2.0.CO;2.

Gitelson, A.A., Zur, Y., Chivkunova, O.B., and Merzlyak, M.N. 2002. "Assessing Carotenoid Content in Plant Leaves with Reflectance Spectroscopy." *Photochemistry and Photobiology*, Vol. 75 (No. 3):pp. 272. doi:10.1562/0031-8655(2002)075<0272:ACCIPL>2.0.CO;2.

Godwin, B., and Thorpe, J. 2002. *Vegetation Management Plan for Saskatchewan Landing Provincial Park*.

Gordon, R., Brown, D. M., and Dixon, M. A. 1994. "Non-destructive estimation of potato leaf area index using a fish-eye radiometer." *Potato Research*, Vol. 37 (No. 4):pp. 393–402. 10.1007/BF02358353.

Goverment of Canada 2022. "Historical climate data."

Gross, Dale, Bell, Scott, Guo, Xulin, Mohammed, 2026. "Detecting crested wheatgrass using sentinel and planetscope time series." *Geomatica*, Vol. 78 (No. 1), p. 100092. doi:10.1016/j.geomat.2026.100092.

Guo, X., Doan, T., Gross, D., and Chu, T. 2020. *Saskatchewan Landing Provincial Park Grassland Management Plan 2020–2030.* Regina, SK, Canada: Saskatchewan Ministry of Parks, Culture and Sport.

Hall, D.B., Anderson, V.J., and Monsen, S.B. 1999. *Competitive effects of bluebunch wheatgrass, crested wheatgrass, and cheatgrass on antelope bitterbrush seedling emergence and survival*, Report No. RMRS-RP-16. Fort Collins, CO, USA: USDA Forest Service, Rocky Mountain Research Station. *USDA Forest Service - Research Papers RMRS*, (No. RMRS-RP-16):pp. 1–7. doi:10.2737/RMRS-RP-16.

Hansen, M. 2006. *Prediction and Management of an Invasive Grass, Agropyron Cristatum*. Ph.D. thesis. Regina, SK, Canada: University of Regina.

Henderson, D. C. 2005. *Ecology and Managment of Crested Wheatgrass Invasion*. Edmonton, AB, Canada: University of Alberta.

Henderson, D.C., and Naeth, M.A. 2005. "Multi-scale impacts of crested wheatgrass invasion in mixed-grass prairie." *Biological Invasions*, Vol. 7 (No. 4):pp. 639–650. doi:10.1007/s10530-004-6669-x.

Hill, M.J. 2013. "Vegetation index suites as indicators of vegetation state in grassland and savanna: An analysis with simulated SENTINEL 2 data for a North American transect." *Remote Sensing of Environment*, Vol. 137 pp. 94–111. doi:10.1016/j.rse.2013.06.004.

Irving, L.J. 2015. "Carbon assimilation, biomass partitioning and productivity in grasses." *Agriculture (Pol'nohospodarstvo)*, Vol. 5 (No. 4):pp. 1116–1134. doi:10.3390/agriculture5041116.

Lobell, D.B., Asner, G.P., Law, B.E., and Treuhaft, R.N. 2001. "Subpixel canopy cover estimation of coniferous forests in Oregon using SWIR imaging spectrometry." *Journal of Geophysical Research: Atmospheres*, Vol. 106 (No. D6):pp. 5151–5160. doi:10.1029/2000JD900739.

Longpre, G. 2024. *Northeast Quadrant Wildfire Risk Assessment and Fuel Management Plan Saskatchewan Landing Provincial Park*. Regina, SK, Canada: Saskatchewan Ministry of Parks, Culture and Sport.

Mallmann, C.L., Pereira Filho, W., Dreyer, J.B.B., Tabaldi, L.A., and Durgante, F.M. 2023. "Leaf-level field spectroscopy to discriminate invasive species (*Psidium guajava* L. and *Hovenia dulcis* Thunb.) from native tree species in the southern Brazilian Atlantic forest." *Remote Sensing*, Vol. 15 (No. 3):pp. 791. doi:10.3390/rs15030791.

Marsett, R.C., Qi, J., Heilman, P., Biedenbender, S.H., Watson, M.C., Amer, S., Weltz, M., Goodrich, D., and Marsett, R. 2006. "Remote sensing for grassland management in the arid Southwest." *Rangeland Ecology & Management*, Vol. 59 (No. 5):pp. 530–540. doi:10.2111/05-201R.1.

Monsen, S. B., Stevens, R., Shaw, N. L., Davis, J. N., Goodrich, S. K., Jorgensen, K. R., Lopez, C. F., *et al.* 2004. *Restoring Western Ranges and Wildlands*, 699–884. USDA Forest Service - General Technical Report RMRS-GTR.

Müllerová, J., Brundu, G., Große-Stoltenberg, A., Kattenborn, T., and Richardson, D.M. 2023. "Pattern to process, research to practice: remote sensing of plant invasions." *Biological Invasions*, Vol. 25 (No. 12):pp. 3651–3676. doi:10.1007/s10530-023-03150-z.

Nafus, A.M., Svejcar, T.J., and Davies, K.W. 2020. "Native Vegetation Composition in Crested Wheatgrass in Northwestern Great Basin." *Rangeland Ecology & Management*, Vol. 73 (No. 1):pp. 9–18. doi:10.1016/j.rama.2019.10.006.

Nafus, A.M., Svejcar, T.J., Ganskopp, D.C., and Davies, K.W. 2015. "Abundances of coplanted native bunchgrasses and crested wheatgrass after 13 years." *Rangeland Ecology & Management*, Vol. 68 (No. 2):pp. 211–214. doi:10.1016/j.rama.2015.01.011.

Nagler, P.L., Inoue, Y., Glenn, E.P., Russ, A.L., and Daughtry, C.S.T. 2003. "Cellulose absorption index (CAI) to quantify mixed soil-plant litter scenes." *Remote Sensing of Environment*, Vol. 87 (No. 2-3):pp. 310–325. (s doi:10.1016/j.rse.2003.06.001.

Ogle, D.E. 2006. "Plant Guide for crested wheatgrass (Agropyron cristatum)." *USDA Plants Database*, last modified 2006, https://plants.sc.egov.usda.gov/DocumentLibrary/plantguide/pdf/pg_agfr.pdf

Ollinger, S.V. 2011. "Sources of variability in canopy reflectance and the convergent properties of plants." *The New Phytologist*, Vol. 189 (No. 2):pp. 375–394. doi:10.1111/j.1469-8137.2010.03536.x.

Operation Grassland Community. 2022. "Managing Crested Wheatgrass in Native Grassland." *Grassland Restoration Forum*, last modified 2022, https://grasslandrestorationforum.ca/wp-content/uploads/2021/03/Sask.-Watershed-Authority-Managing-Crested-Wheatgrass…-.pdf

Pellant, M., and Lysne, C. R. 2005. "Strategies to Enhance Plant Structure and Diversity in Crested Wheatgrass Seedings." USDA Forest Service Proceedings, pp. 81–92.

Penuelas, J., Baret, F., and Filella, I. 1995. "Semi-empirical indices to assess carotenoids/chlorophyll a ratio from leaf spectral reflectance." *Photosynthetica*, Vol. 31 (No. 2):pp. 221–230.

Pérez-Harguindeguy, N., Díaz, S., Garnier, E., Lavorel, S., Poorter, H., Jaureguiberry, P., Bret-Harte, M.S., *et al.* 2016. "Corrigendum to: New handbook for standardised measurement of plant functional traits worldwide." *Australian Journal of Botany*, Vol. 64 (No. 8):pp. 715–716. (doi:10.1071/BT12225_CO.

Planet. 2025. "PlanetScope Spectral Response Functions (PS-SRF)." *Planet Labs*, last modified 2025, https://docs.planet.com/data/imagery/planetscope/

Pu, Y., Nixon, A., Prieto, B., and Guo, X. 2025. "Identifying native grasslands and key phenological stages using time series Sentinel-2 data and deep learning models." *International Journal of Applied Earth Observation and Geoinformation*, Vol. 140 (No. May):pp. 104619. doi:10.1016/j.jag.2025.104619.

R Core Team 2017."R: A Language and Environment for Statistical Computing". *R Foundation for Statistical Computing,* https://www.R-project.org/

Rakotoarivony, M.N.A., Gholizadeh, H., Hammond, W.M., Hassani, K., Joshi, O., Hamilton, R.G., Fuhlendorf, S.D., Trowbridge, A.M., and Adams, H.D. 2023. "Detecting the invasive Lespedeza cuneata in grasslands using commercial small satellite imagery." *International Journal of Remote Sensing*, Vol. 44 (No. 21):pp. 6802–6824. doi:10.1080/01431161.2023.2275321.

Rakotoarivony, M.N.A., Gholizadeh, H., Hassani, K., Zhai, L., and Rossi, C. 2025. "Mapping the spatial distribution of species using airborne and spaceborne imaging spectroscopy: A case study of invasive plants." *Remote Sensing of Environment*, Vol. 318 (No. December 2024):pp. 114583. doi:10.1016/j.rse.2024.114583.

Rockwell, S.M., Wehausen, B., Johnson, P.R., Kristof, A., Stephens, J.L., Alexander, J.D., and Barnett, J.K. 2021. "Sagebrush bird communities differ with varying levels of crested wheatgrass invasion." *Journal of Fish and Wildlife Management*, Vol. 12 (No. 1):pp. 27–39. doi:10.3996/JFWM-20-035.

Rogler, G.A., and Lorenz, R.J. 1983. "Crested Wheatgrass: Early History in the United States." *Journal of Range Management*, Vol. 36 (No. 1):pp. 91. doi:10.2307/3897991.

Sahoo, R.N., Ray, S.S., and Manjunath, K.R. 2015. "Hyperspectral remote sensing of agriculture." *Current Science*, 108: 848–859.

Saskatchewan Ministry of Parks Culture and Sports 2021. Saskatchewan Parks Boundaries [WWW Document]. https://open.canada.ca/data/dataset/65f14e41-c6c7-512e-e231-aa1079978b12 (accessed 2.2.25).

Schroeder, V., and Johnson, D. 2019. Bunchgrass Phenology [WWW Document]. https://extension.oregonstate.edu/catalog/em-9276-bunchgrass-phenology-using-growth-stages-grasses-adaptive-grazing-management-tools.

Serrano, L., Peñuelas, J., and Ustin, S.L. 2002. "Remote sensing of nitrogen and lignin in Mediterranean vegetation from AVIRIS data: Decomposing biochemical from structural signals." *Remote Sensing of Environment*, Vol. 81 (No. 2-3):pp. 355–364. doi:10.1016/S0034-4257(02)00011-1.

Sims, D.A., and Gamon, J.A. 2002. "Relationships between leaf pigment content and spectral reflectance across a wide range of species, leaf structures and developmental stages." *Remote Sensing of Environment*, Vol. 81 (Nos. 2-3):pp. 337–354. doi:10.1016/S0034-4257(02)00010-X.

Soubry, I., and Guo, X. 2021. "Identification of the optimal season and spectral regions for shrub cover estimation in Grasslands." *Sensors (Basel, Switzerland)*, Vol. 21 (No. 9):pp. 3098. doi:10.3390/s21093098.

Tandoh, S. 2019. *Characterization of crested wheatgrass germplasms for plant maturity and associated physiological and morphological traits*. M.Sc. thesis. Saskatoon, Canada: University of Saskatchewan.

Taylor, S.L., Hill, R.A., and Edwards, C. 2013. "Characterising invasive non-native Rhododendron ponticum spectra signatures with spectroradiometry in the laboratory and field: Potential for remote mapping." *ISPRS Journal of Photogrammetry and Remote Sensing*, Vol. 81 pp. 70–81. doi:10.1016/j.isprsjprs.2013.04.003.

Thenkabail, P., Lyon, J., Huete, A., Thenkabail, A., Lyon, P., and Huete, J. 2013. "Hyperspectral remote sensing of vegetation and agricultural crops." *Photogrammetric Engineering and Remote Sensing*, 80(4): 697–709.

Thorpe, J. 2007. *Saskatchewan Rangeland Ecosystems: Ecoregions and Ecosites*. Saskatchewan, Canada: Saskatchewan Research Council.

Thorpe, J. 2014. *Saskatchewan Rangeland Ecosystems Publication 1: Ecoregions and Ecosites (Version 2) - A project of the Saskatchewan Prairie Conservation Action Plan*. Saskatchewan, Canada: Saskatchewan Research Council.

Tu, Y.H., Johansen, K., Aragon, B., El Hajj, M.M., and McCabe, M.F. 2022. "The radiometric accuracy of the 8-band multi-spectral surface reflectance from the planet SuperDove constellation." *International Journal of Applied Earth Observation and Geoinformation*, Vol. 114 (No. September):pp. 103035. doi:10.1016/j.jag.2022.103035.

Urness, P.J., Austin, D.D., and Fierro, L.C. 1983. "Nutritional value of crested wheatgrass for wintering mule deer." *Journal of Range Management*, Vol. 36 (No. 2):pp. 225. doi:10.2307/3898168.

Vaness, B. 2008. *Heterogeneity of roots and resources in crested wheatgrass (Agropyron cristatum) and native prairie grasses*. MSc Thesis. Regina, Saskatchewan, Canada. University of Regina.

Vaness, B.M., and Wilson, S.D. 2007. "Impact and management of crested wheatgrass (Agropyron cristatum) in the northern Great Plains." *Canadian Journal of Plant Science*, Vol. 87 (No. 5):pp. 1023–1028. doi:10.4141/CJPS07120.

Vojtech, E., Turnbull, L.A., and Hector, A. 2007. "Differences in Light Interception in Grass Monocultures Predict Short-Term Competitive Outcomes under Productive Conditions." *PloS One*, Vol. 2 (No. 6):pp. e499. doi:10.1371/journal.pone.0000499.

Weisberg, P.J., Dilts, T.E., Greenberg, J.A., Johnson, K.N., Pai, H., Sladek, C., Kratt, C., Tyler, S.W., and Ready, A. 2021. "Phenology-based classification of invasive annual grasses to the species level." *Remote Sensing of Environment*, Vol. 263 (No. June):pp. 112568. doi:10.1016/j.rse.2021.112568.

Wu, W., Chen, L., Liang, R., Huang, S., Li, X., Huang, B., Luo, H., Zhang, M., Wang, X., and Zhu, H. 2024. "The role of light in regulating plant growth, development and sugar metabolism: a review." *Frontiers in Plant Science*, Vol. 15 (No. January):pp. 1507628. doi:10.3389/fpls.2024.1507628.

Xu, D., Liu, Y., Xu, W., and Guo, X. 2022. "The impact of NPV on the spectral parameters in the yellow-edge, red-edge and NIR shoulder wavelength regions in grasslands." *Remote Sensing*, Vol. 14 (No. 13):pp. 3031. doi:10.3390/rs14133031.

Yu, X., Guo, Q., Chen, Q., and Guo, X. 2019. "Discrimination of senescent vegetation cover from Landsat-8 OLI Imagery by spectral unmixing in the northern mixed grasslands." *Canadian Journal of Remote Sensing*, Vol. 45 (No. 2):pp. 192–208. doi:10.1080/07038992.2019.1605586.

Zapisocki, Z., Murillo, R. d A., and Wagner, V. 2022. "Non-native plant invasions in prairie Grasslands of Alberta, Canada." *Rangeland Ecology & Management*, Vol. 83 pp. 20–30. doi:10.1016/j.rama.2022.02.011.

Zheng, Q., Huang, W., Cui, X., Shi, Y., and Liu, L. 2018. "New spectral index for detecting wheat yellow rust using sentinel-2 multispectral imagery." *Sensors (Basel, Switzerland)*, Vol. 18 (No. 3):pp. 1–19. doi:10.3390/s18030868.

Zhou, W. 2007. Assessing Remote Sensing Application on Rangeland. M.Sc. thesis. Saskatoon, Saskatchewan, Canada: University of Saskatchewan.